NASA TECHNICAL NOTE

NASA TN D-3867

NASA TN D-3867

STATIC CALIBRATION OF AN EJECTOR UNIT FOR SIMULATION OF JET ENGINES IN SMALL-SCALE WIND-TUNNEL MODELS

by Richard J. Margason and Garl L. Gentry

Langley Research Center
Langley Station, Hampton, Va.

NATIONAL AERONAUTICS AND SPACE ADMINISTRATION • WASHINGTON, D. C. • MARCH 1967

STATIC CALIBRATION OF AN EJECTOR UNIT FOR SIMULATION OF JET ENGINES IN SMALL-SCALE WIND-TUNNEL MODELS

By Richard J. Margason and Garl L. Gentry

Langley Research Center
Langley Station, Hampton, Va.

NATIONAL AERONAUTICS AND SPACE ADMINISTRATION

For sale by the Clearinghouse for Federal Scientific and Technical Information
Springfield, Virginia 22151 – CFSTI price $3.00

STATIC CALIBRATION OF AN EJECTOR UNIT FOR SIMULATION OF JET ENGINES IN SMALL-SCALE WIND-TUNNEL MODELS

By Richard J. Margason and Garl L. Gentry
Langley Research Center

SUMMARY

This report describes an ejector that was developed to simulate performance characteristics of a jet engine in small-scale wind-tunnel models. The thrust produced by the simulator and the secondary (inlet) mass flow were calibrated statically as a function of the total- and static-pressure measurements inside the ejector nozzle. The thrust can be repeated within 1 percent for a given set of pressure measurements. Deflections of the exit up to 30^{o} changed only the angle of the resultant thrust.

The ratio of the thrust to secondary (inlet) mass flow was used as a scale factor for the static simulation of jet-engine performance. This scale factor can be changed either by changing the level of thrust (varying the primary line pressure) or by changing the nozzle exit area. Wind-tunnel models that use these ejectors should have levels of jet-induced lift loss which are comparable to those caused by a jet engine.

INTRODUCTION

The design of jet VTOL aircraft requires a detailed knowledge of thrust losses and interference effects caused by jet engines installed in the aircraft. These include inlet losses, lift losses, hot-gas ingestion losses, jet-induced pitching-moment increment, effects on stability and control, and ground effects. This report describes an ejector that was developed to simulate performance characteristics of a full-scale jet engine in small-scale wind-tunnel models so that some of the above effects could be measured.

The ejector (figs. 1 and 2) was sized for use with wind-tunnel models in the 17-foot (5-meter) test section of the Langley 300-MPH 7- by 10-foot tunnel. Since the ejector is powered by compressed air, it cannot simulate the exhaust temperature of a jet engine. However, for most aerodynamic testing, it appears that the primary variables that must be properly simulated are the jet thrust, exit area, and inlet mass flow (ref. 1). The ejector is capable of simulating these variables, since inlet mass flow and the jet thrust can both be controlled by varying the pressure of the primary air supply. The ratio of jet thrust to inlet mass flow found in jet engines can be used as a parameter for scaling the static performance of the ejector. This ratio ranges from 55 to 65 lbf/lbm/sec

(540 to 640 N/kg/sec) for existing turbojet engines; for fan-type jet engines this ratio may be as low as 35 lbf/lbm/sec (340 N/kg/sec); and for proposed lift-jet engines it may be as high as 90 lbf/lbm/sec (883 N/kg/sec). Descriptions of other ejector configurations for simulating jet engines at small scale are presented in references 2 and 3.

The ejector unit described in reference 2 is slightly larger in diameter than the ejector in figure 1(a) and approximately three times as long. Since lower pressure is used for the primary air supply in the ejector of reference 2, the maximum thrust level is about one-third less and the scale parameter is about 40 percent less than for the ejector in figure 1(a); as a result, the ejector in reference 2 cannot simulate existing turbojet engines. The ejector unit described in reference 3 was designed and built to fit in a particular model and does not lend itself to application in other models without drastic redesign. The maximum thrust of the ejector is less than one-third that of the ejectors described in this report.

The basic jet simulator in figure 1(a) was designed to produce up to 70 lbf of thrust per lbm/sec inlet mass flow (690 N/kg/sec) with a 2-inch-diameter (5.08-cm) exit nozzle and was required to fit in the volume of a $3\frac{1}{2}$-inch (8.89-cm) cube. The purpose of this investigation was to obtain a static calibration of these ejectors to evaluate their performance and to determine the effects of changing the exit area, the mixing length, the jet dynamic-pressure decay, the jet nozzle configuration, and the jet nozzle vectoring.

SYMBOLS

The units used for the physical quantities defined in this paper are given both in U.S. Customary Units and in the International System of Units (SI). Factors relating these two systems of units are presented in reference 4. The symbols used are defined as follows:

A_j area of the exit nozzle for the basic ejector configuration, 3.142 in^2 (20.272 cm^2)

A_p total throat area of the 177 primary convergent-divergent nozzles, 0.131 in^2 (0.845 cm^2)

D diameter of the jet-nozzle exit for the basic ejector configuration, 2.000 in. (5.080 cm)

F measured resultant jet thrust, lbf (N)

F_c compressibility factor

F_i	ideal jet thrust, based on complete isentropic expansion of the ideal exit mass flow, lbf (N)
ΔL	load induced on plate, lbf (N)
p	atmospheric pressure, psi (N/m^2)
p_l	line pressure at entrance to ejector plenum chamber, psi (N/m^2)
$p_{s,e}$	static pressure measured in the exit plane of the jet nozzle, psi (N/m^2)
$p_{s,r}$	static pressure measured by the rake in the jet nozzle, psi (N/m^2)
p_t	total pressure, psi (N/m^2)
$p_{t,e}$	total pressure measured in the exit plane of the jet nozzle, psi (N/m^2)
$p_{t,r}$	total pressure measured by the rake in the jet nozzle, psi (N/m^2)
q_e	average dynamic pressure in the exit plane of the jet nozzle, psi (N/m^2)
q_z	peak dynamic pressure measured at a distance z downstream from the jet-nozzle exit plane, psi (N/m^2)
R	radius of the jet nozzle of the basic ejector configuration, 1.00 in. (2.540 cm)
r	local radius measured from the center line of the jet nozzle, in. (cm)
S	plate planform area, in^2 (cm^2)
w_p	primary mass flow; the total mass flow of compressed air used to drive the ejector, lbm/sec (kg/sec)
w_s	secondary mass flow; the mass flow induced through the ejector inlet by the primary nozzles, lbm/sec (kg/sec)
z	distance measured downstream from the jet nozzle, in. (cm)
δ	deflection angle of the jet nozzle, deg (rad)
θ	deflection angle of the measured resultant jet thrust, deg (rad)

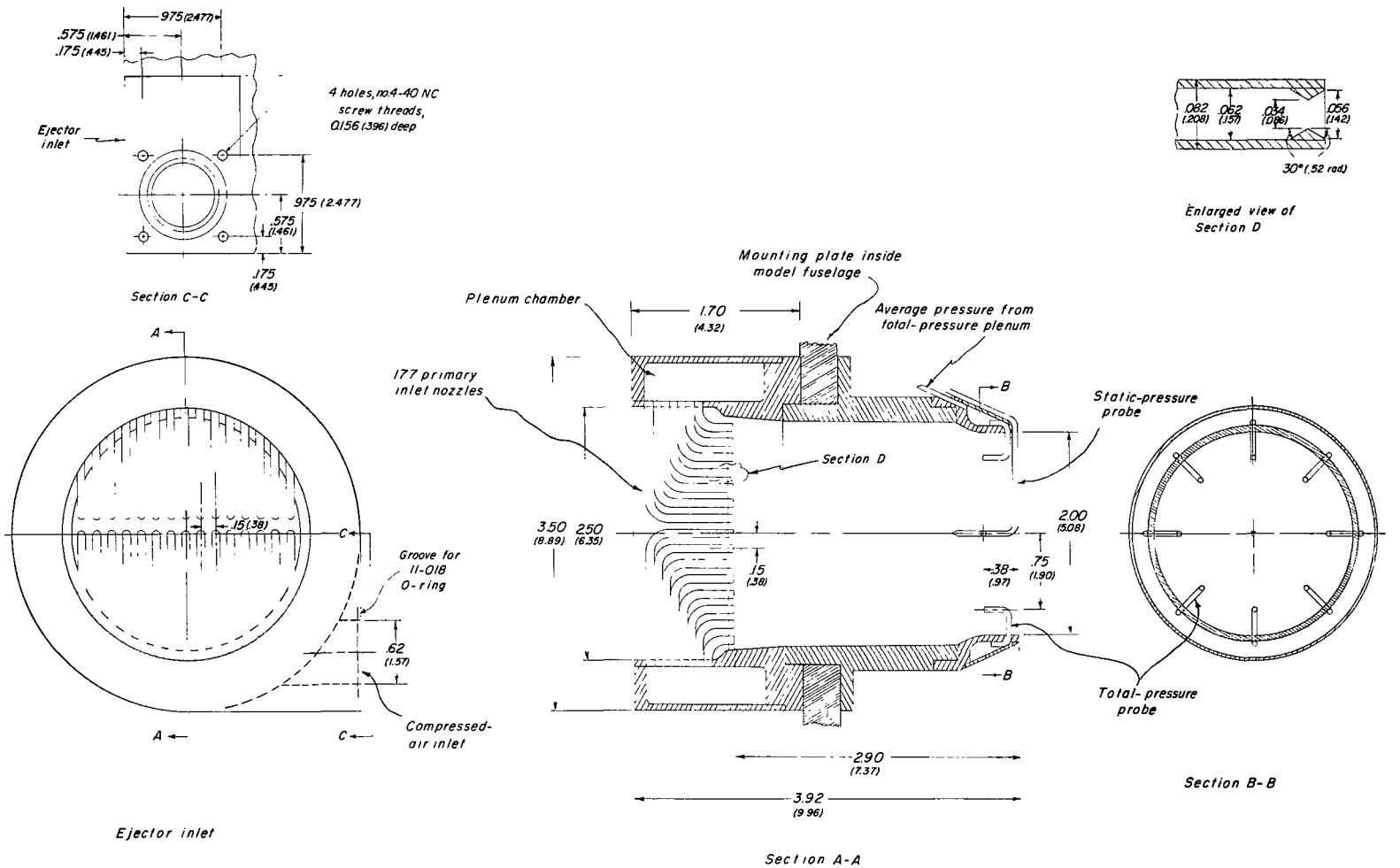

(a) The basic ejector configuration for simulating lift-jet engines. Dimensions are in inches (centimeters).

Figure 1.- Section views of ejector configurations.

MODEL AND APPARATUS

Drawings of the jet-engine simulator in two different configurations are shown in figure 1. Figure 1(a) shows the basic ejector configuration for simulating lift-jet engines; photographs of this configuration are presented in figure 2. The first part of the section entitled "Discussion and Results" gives the characteristics of this configuration. Figure 1(b) shows a second ejector configuration which may be used to simulate a lift-cruise engine in the deflected position. The jet-engine simulator can be broken into three major components: the ejector unit, a removable mixing chamber, and an exit rake and nozzle. The ejector unit is basically a plenum chamber which supplies compressed air at pressures up to 350 psig (2.41 MN/m^2) to 177 convergent-divergent nozzles (fig. 2(b)). This large number of primary nozzles was used to reduce the distortion of the total-pressure profile at the exit plane of the jet nozzle. Section D in figure 1(a) gives the dimensions of one of the convergent-divergent nozzles. These nozzles produce the primary ejector mass flow which induces a secondary flow through the ejector inlet. This secondary flow represents the engine inlet mass flow. The second major component is the mixing

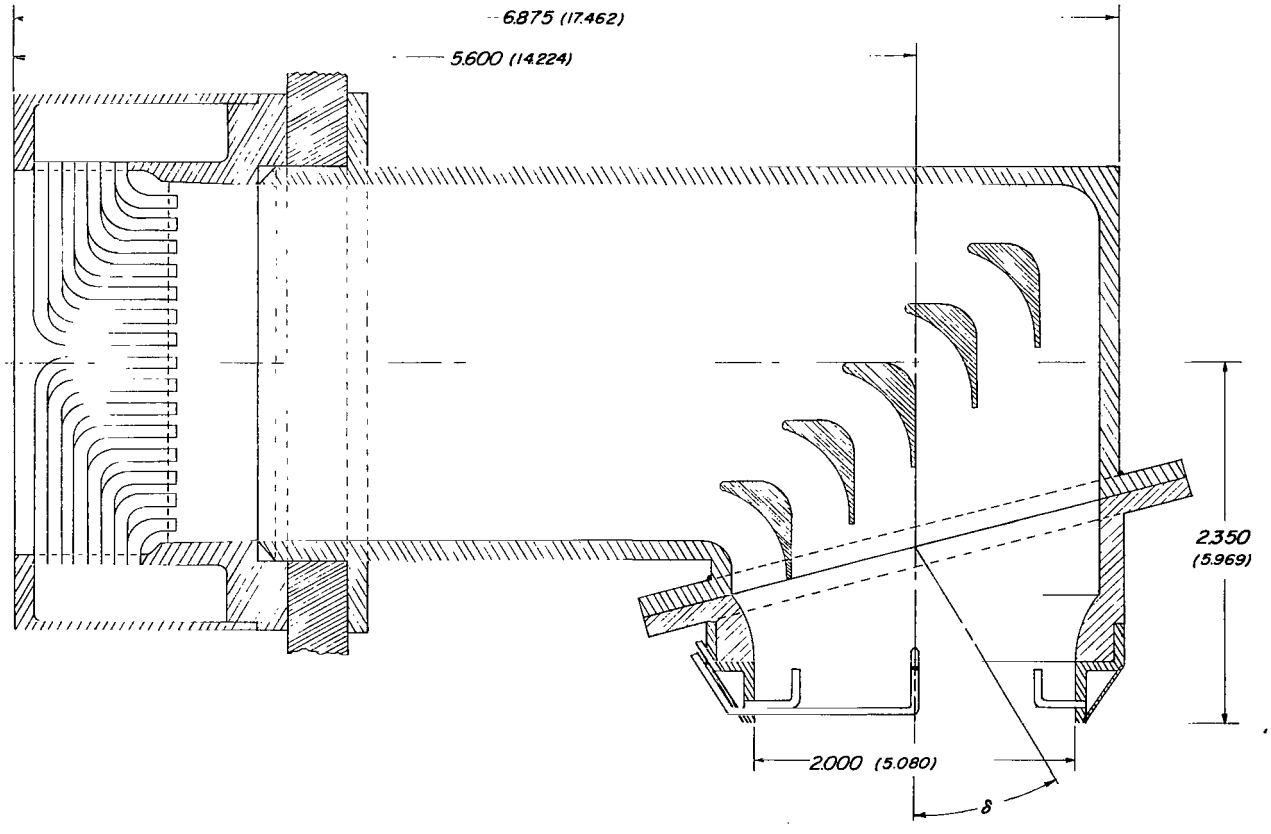

(b) The configuration for simulating lift-cruise engines deflected 90^0. Dimensions are in inches (centimeters).

Figure 1.- Concluded.

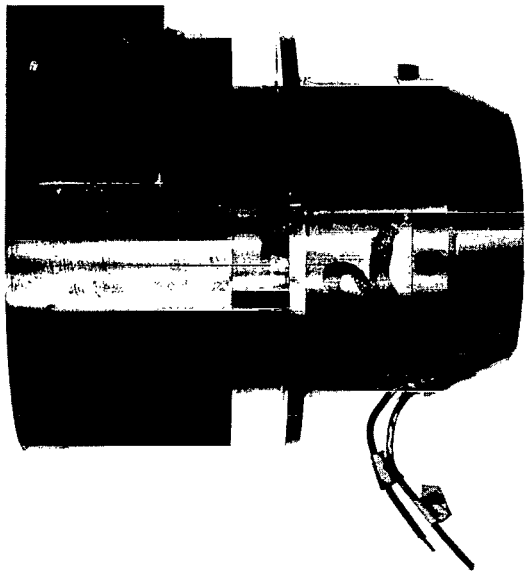

L-66-5159

(a) Basic ejector configuration for simulating lift-jet engines.

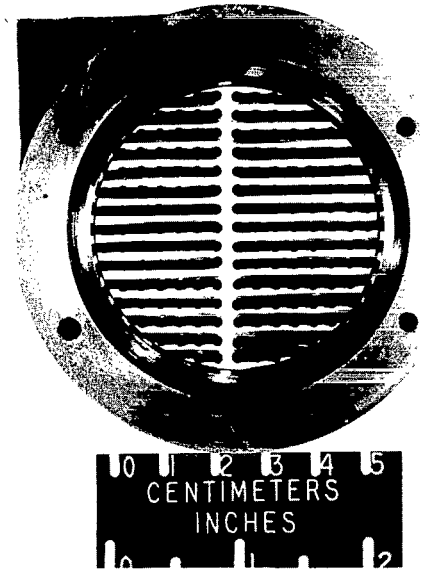

L-66-5161

(b) View of the 177 convergent-divergent nozzles from the inside of the ejector looking toward the ejector inlet.

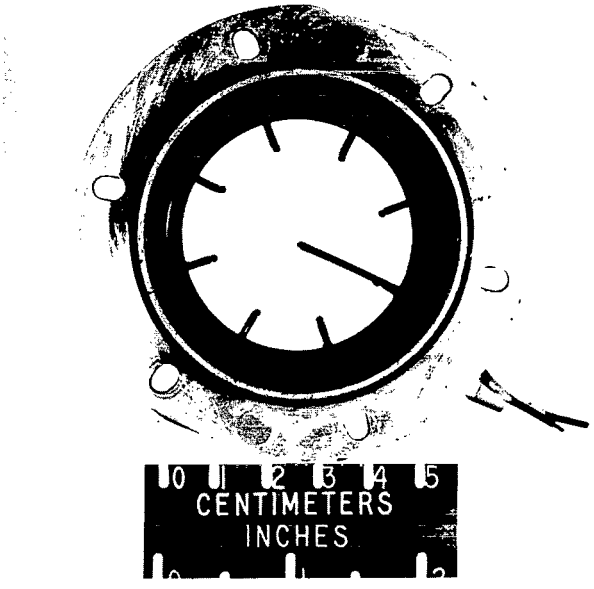

L-66-5160

(c) View of the exit rake from the inside looking toward the nozzle exit.

Figure 2.- Photographs of lift-jet engine configuration.

chamber, which may be straight as shown in figure 1(a) or may be extended and deflected as shown in figure 1(b). The third major component, the exit rake and nozzle, is shown in section B-B of figure 1(a) and in figure 2(c). The rake consists of eight total-pressure probes which connect to a common plenum in the wall of the exit nozzle to provide an average value of total pressure. A single static-pressure probe is located at the center of the nozzle. This combination gives a pressure difference $(p_{t,r} - p_{s,r})$ that is proportional to the dynamic pressure of the jet which in turn is proportional to the jet thrust. Strain-gage balance arrangements were considered for the thrust measurement when the ejector was being designed, but they were found to be far more complex than the pressure-measuring method.

The results presented in this report are based on measurements made statically with the jet-engine simulator mounted on a test stand supported by a three-component strain-gage balance as shown in figure 3. The balance measured normal force, axial force, and pitching moment. Compressed air was supplied to the ejector unit by a 1/2-inch-diameter (1.27-cm) thin-wall inconel tube which was mounted across the strain-gage balance to form a limber spring. This method puts a very small but repeatable tare load on the balance which is included in the balance calibration. The thrust presented in these data represents the resultant force based on the normal-force and axial-force measurements. The net turning angles presented were also determined from these measurements.

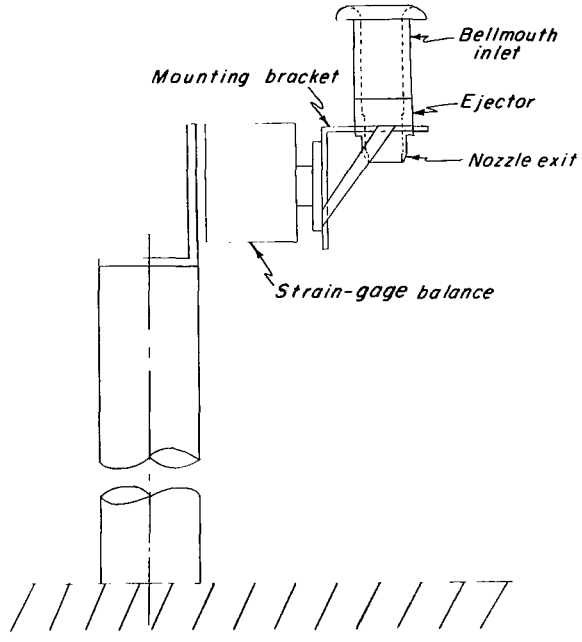

Figure 3.- Sketch showing the ejector mounted on the three-component balance for static calibration.

Additional measurements were made to determine the primary and secondary mass flow, the pressure profiles in the jet-nozzle exit plane, the total-pressure profiles downstream of the jet nozzle exit, and the induced loads on surfaces adjacent to the jet-nozzle exit. The primary mass flow was measured by a 1/2-inch-diameter (1.27-cm) venturi flowmeter in the compressed-air supply line. The secondary mass flow was determined from static pressures measured in the bellmouth inlet shown in figure 3. The total-pressure profiles at the jet-nozzle exit plane and farther downstream were measured on a mercury manometer. The induced loads were measured on circular plates which were mounted by means of beams fitted with strain gages. A similar arrangement is shown in figure 7 of reference 5.

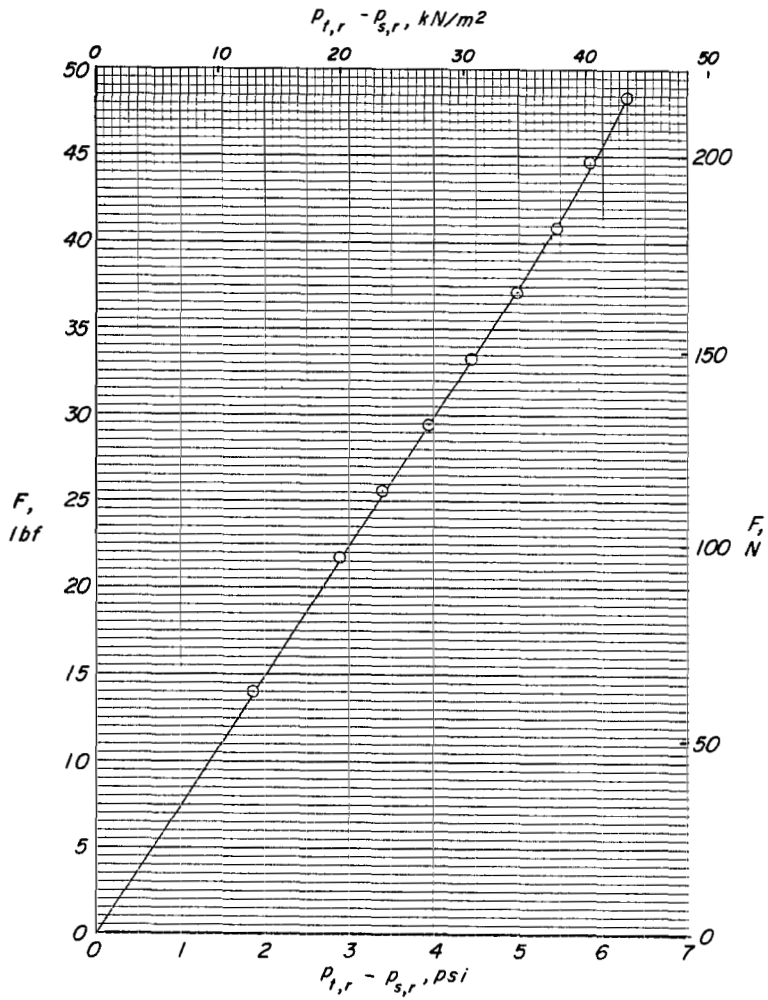

Figure 4.- Typical calibration of jet thrust as function of pressure difference inside the nozzle.

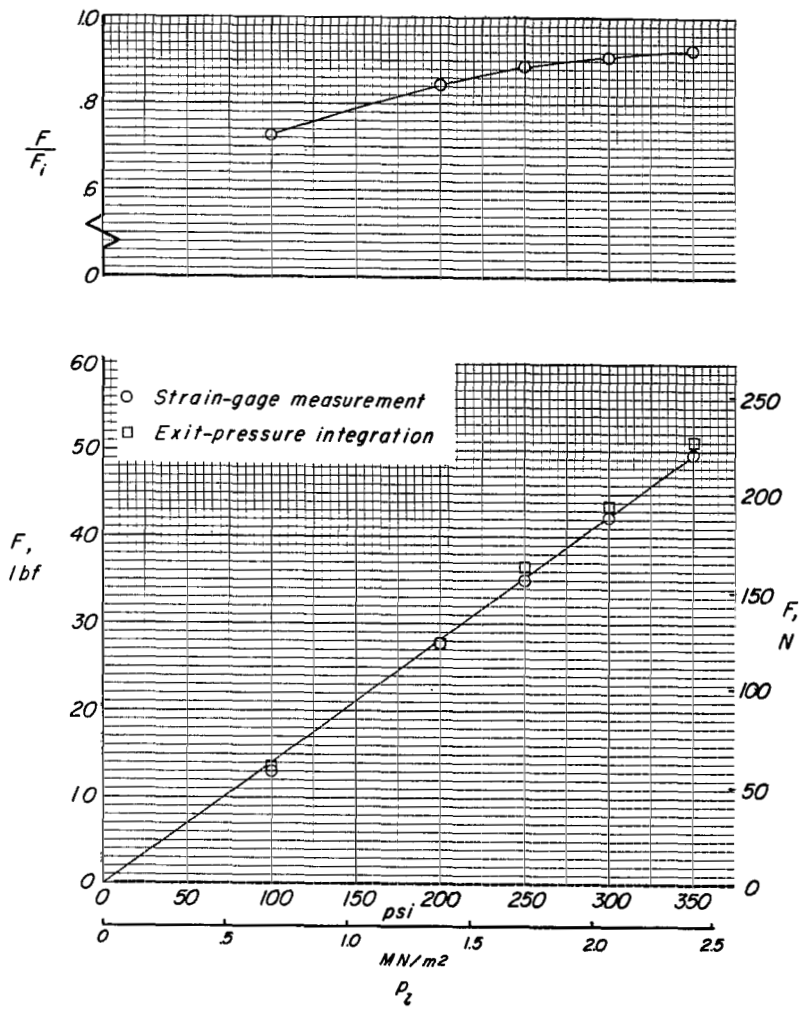

Figure 5.- Comparisons of thrust measured by strain gages with thrust determined by exit-pressure integration and with ideal thrust.

Since one of the primary purposes of this investigation was to evaluate the use of this type of ejector as a thrust-producing device, some preliminary tests were conducted to evaluate the thrust-measuring method. Calibration curves were prepared (fig. 4), with static thrust plotted as a function of the difference between the average total pressure and the static pressure measured on the test stand by means of the strain-gage balance. The jet thrust obtained in wind-tunnel tests can be determined from the pressure difference measured by the rake with an equation obtained from a polynomial curve fit for the calibration curve. To determine the sensitivity of the calibration curve to changes in simulator configuration, a single ejector was tested with three different exit nozzles. The largest difference in the calibration curves for these three configurations was a variation of 8 percent in thrust for a given value of pressure difference $\left(p_{t,r} - p_{s,r}\right)$. This variation resulted from differences in the values of static pressure measured by the exit rake. The ports in the first static-pressure probe were farther inside the nozzle exit than the ports in the other two exit rakes. Since the nozzle converges, the measurements would be expected to change with these changes in location. A comparison was also made of calibration curves obtained from four different ejector units, each with the same exit nozzle and instrumentation. The results gave calibrations that differed by as much as 6 percent, thus indicating differences in the performance of the ejectors. These two sets of calibrations, therefore, demonstrate the need for calibrating each ejector and exit combination. Repeat calibrations of a single ejector and nozzle exit combination agreed within 1 percent.

As a further verification of the calibration, the thrust of the ejector was measured by two methods: a strain-gage balance and an exit-plane pressure profile. Both measurements were made at the same time. The area between the exit total-pressure curve and the exit static-pressure curve was integrated for several values of line pressure to obtain the thrust. As shown in figure 5, these values of thrust are up to 3 percent higher than the thrust measured by the strain-gage balance. This difference is attributed to the uneven total-pressure profile and is rather small considering the difficulty encountered in measuring and integrating these data accurately. Also presented in figure 5 is the ratio of strain-gage-measured thrust to ideal thrust based on complete isentropic expansion of the ideal mass flow at the pressure ratio measured in the jet-nozzle exit. This ratio is presented as a measure of the nozzle efficiency. The total-pressure profile measured at the exit plane of the nozzle for a primary air supply pressure of 250 psig (1.72 MN/m^2) is presented in figure 6. These results are compared with an equivalent value of pressure computed from the balance thrust measurement by the following equation:

$$p_{t,e} - p_{s,e} = \frac{F_c F}{2A_j}$$

DISCUSSION AND RESULTS

The purpose of this investigation was twofold: (1) to determine the performance characteristics of the basic ejector configuration shown in figures 1 and 2, and (2) to determine the effect of several variations in this basic ejector configuration. Accordingly the results are presented in two parts.

Performance Characteristics of the Basic Ejector

The investigation of the basic ejector configuration (figs. 1(a) and 2) was concerned with the following performance characteristics: thrust, line pressure of the compressed air at the plenum-chamber inlet, primary (compressed air) mass flow, secondary (inlet) mass flow, nozzle-exit pressure profiles, jet efflux dynamic-pressure decay, and jet-induced lift loss. The most significant performance characteristic, thrust, and the calibration curve (fig. 4) have already been discussed in the previous section. It should be emphasized that these curves vary slightly from one ejector to another because of the limitations discussed previously. This calibration curve (fig. 4) represents only a typical variation of thrust with pressure difference inside the nozzle. It should be noted that both the total pressure and the static pressure were measured approximately 0.4 inch (1 cm) inside the nozzle exit plane and do not represent the exit pressures.

Nozzle-exit pressure profiles.- The nozzle-exit total-pressure profile of the lift-jet engine simulator configuration presented in figure 6 is not uniform. The exact profile varies over the plane of the nozzle exit and depends on the particular traverse selected across the exit. These data represent the best average of pressures measured at 48 different locations in the exit plane. Total-pressure profiles for existing lift-jet engines are not available for comparison. Generally, profiles for turbojet engines are nonuniform because of the fairing behind the turbine, which forms a centerbody ahead of the nozzle exit. Consequently, the shape of the ejector-exit pressure profile is somewhat similar to that of a turbojet engine.

Jet dynamic-pressure decay.- In reference 5, it was shown that the jet dynamic-pressure decay determines the induced lift losses for hovering out of ground effect. To determine this parameter, dynamic-pressure profiles were measured at several stations downstream of the exit plane (fig. 7). The decay is based on the peak values of dynamic pressure at each of the downstream stations. The local peak values of dynamic pressure have been divided by the average value of dynamic pressure in the exit plane shown in figure 6. These nondimensional values have been plotted as a function of distance downstream of the nozzle in figure 8(a). It should be noted that the decay curve for the lift-jet engine simulator is almost identical with that for the convergent nozzle using compressed air from a cylindrical plenum chamber presented in reference 5. Also shown for comparison are data from a J-85 jet engine (ref. 6).

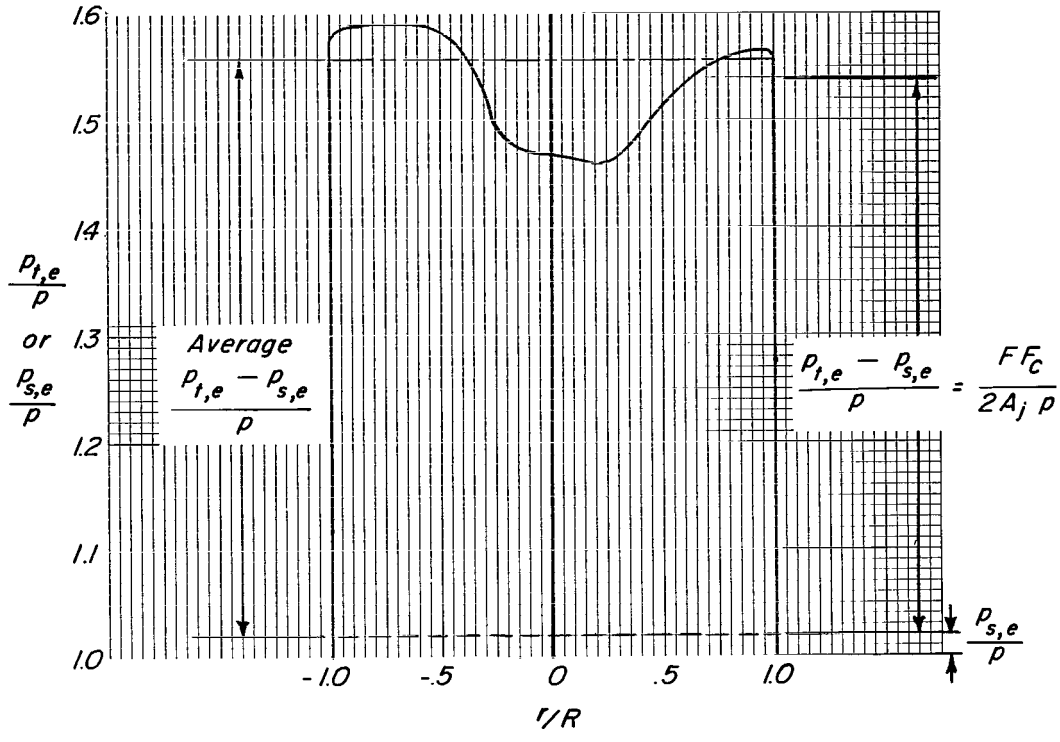

Figure 6.- Exit pressure distribution of an ejector at a drive pressure of 250 psig (1.72 MN/m^2).

Lift loss induced by the jet.- The jet-induced lift losses were then measured on circular plates mounted in the plane of the nozzle exit by means of three beams fitted with strain gages. This arrangement, sketched at the top of figure 8(b), is the same as that used in reference 5 with the cylindrical plenum chamber. Figure 8(b) shows agreement of induced lift loss among three sets of data: lift-jet engine simulator, convergent nozzle, and J-85 jet engine. Therefore, wind-tunnel models that use these ejectors to simulate jet engines should have the same levels of jet-induced lift loss as would be caused by the jet engine in reference 6.

Primary and secondary mass flow.- Some additional performance characteristics for a particular lift-jet engine simulator are presented in figure 9. While the exact values vary from one ejector to another, these data are typical. As would be expected, the primary (compressed air) mass flow and the line pressure p_l are both linear functions of the pressure difference measured by the exit rake. The pressure drops sharply as the compressed air flows from the plenum chamber through the tubes to the primary nozzles and then mixes with the secondary air flow. This is indicated by the values of the pressure measurements at the ejector (fig. 6).

The secondary mass flow increases rapidly at low values of the pressure difference measured by the rake and then levels off above 4.5 psig (31.5 kN/m^2). This flattening of

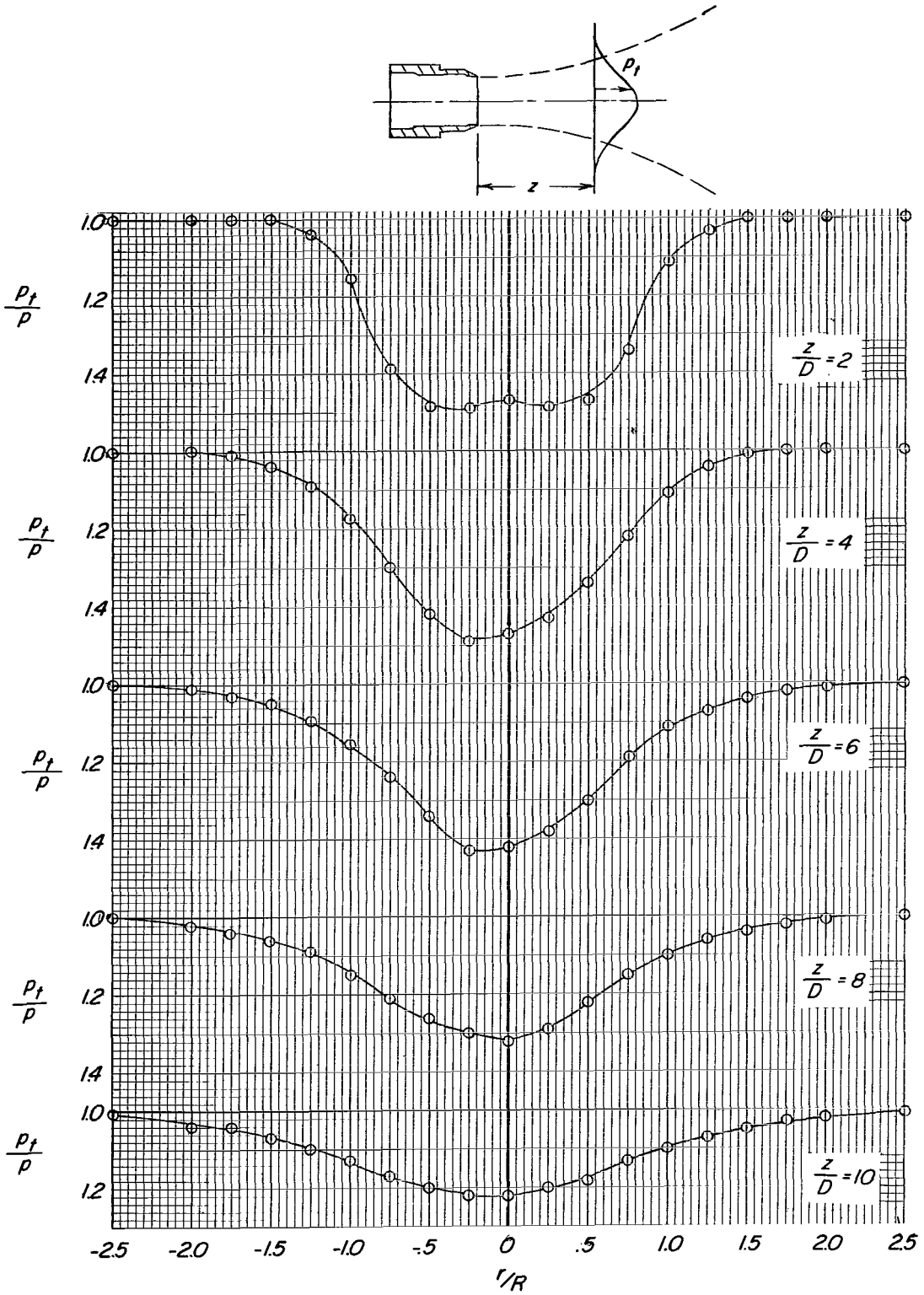

Figure 7.- Total-pressure profiles downstream of the nozzle exit.

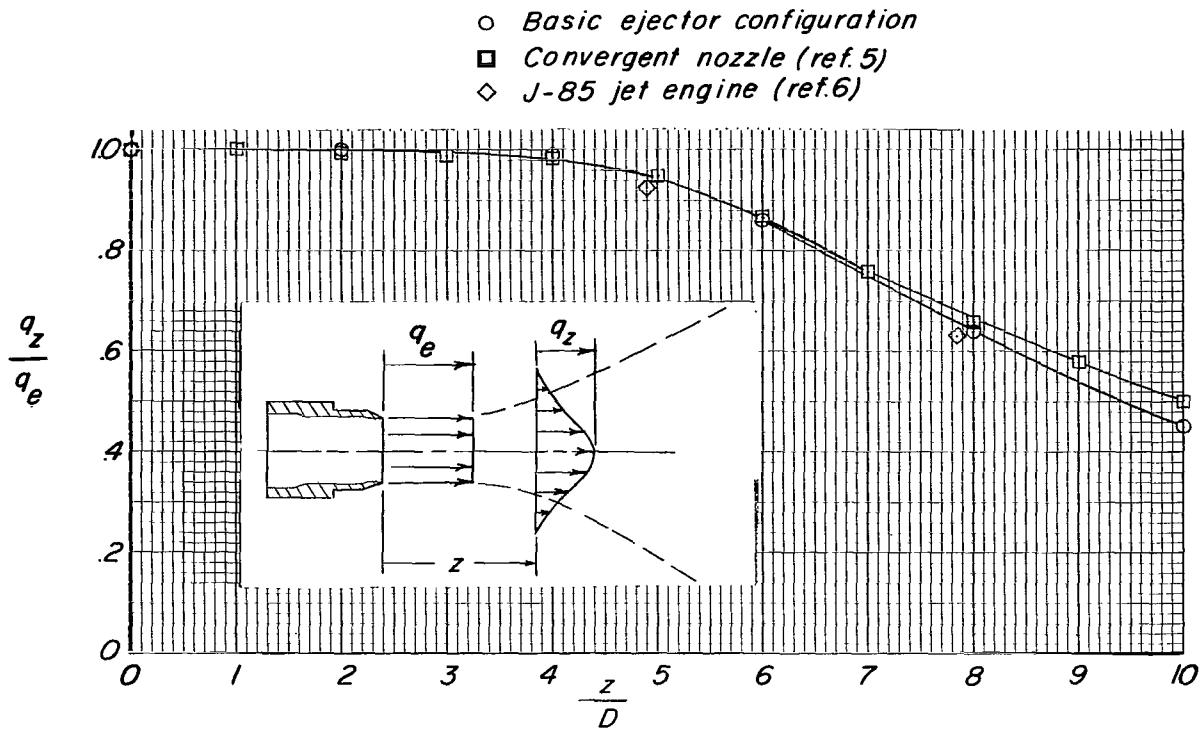

(a) Dynamic-pressure decay.

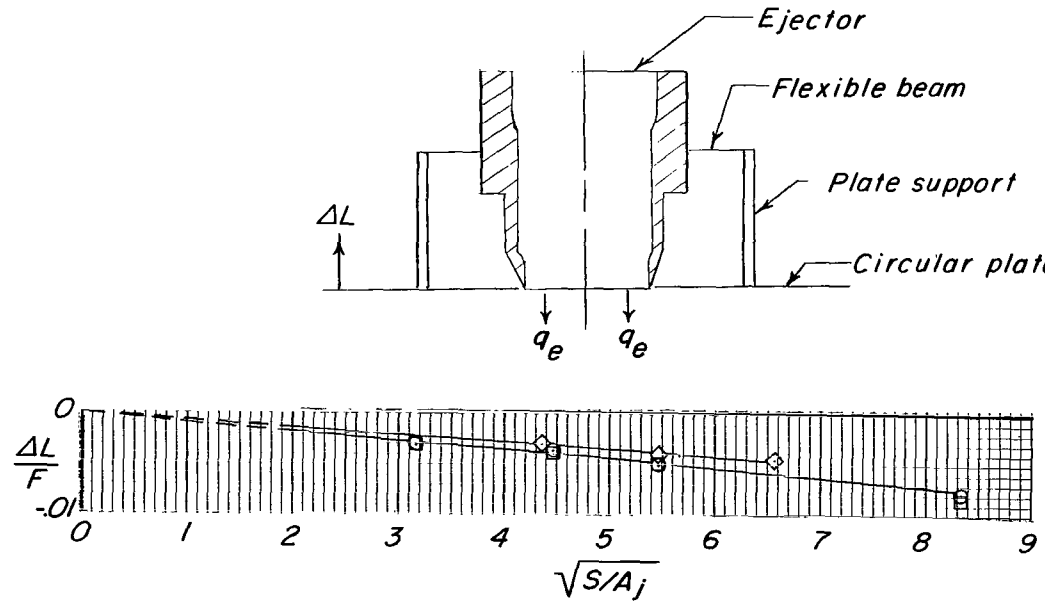

(b) Induced lift loss.

Figure 8.- Comparison of ejector-induced lift loss and dynamic-pressure decay with other data.

the curve is believed to be due to choking of the inlet flow. The primary flow is supersonic and underexpanded; thus it tends to induce high velocities and reduce the effective cross-sectional area of the secondary flow downstream of the primary-nozzle exits. The choked flow could also occur in the region of the tubes supplying the primary nozzles. For the measured level to be the result of choked flows in this region, the effective cross-sectional area would have to be about one-third the physical cross-sectional area. In the ejector section, large surfaces are present for boundary-layer and flow separation. Also, this section is not a uniformly converging nozzle. These features combine to produce an inlet with an extremely low efficiency; that is, they drastically reduce the effective cross-sectional area. Since the flow in this region of the ejector is so complex, no attempt was made to verify the presence of these conditions experimentally. A theoretical and experimental investigation of the flow inside a much simpler ejector arrangement has been conducted and is discussed in reference 7.

Scale factor for jet-engine simulation.- Proper simulation of all the operating parameters of a jet engine is not possible with an ejector powered by compressed air. For example, the jet efflux temperature of a jet engine is not simulated. Previous work (refs. 1, 2, and 3) has shown that one of the most important parameters of the efflux is the rate of discharge of momentum (jet thrust) and the most important parameter at the inlet is the mass flow. To obtain a single factor to scale the simulation of these two parameters by the jet-engine simulator for static conditions, a ratio of jet thrust to inlet mass flow has been used. This is shown in figure 9, where the scale factor F/w_s is plotted as a function of $p_{t,r} - p_{s,r}$. This scale factor ranges from about 55 to 65 lbf/lbm/sec (540 to 640 N/kg/sec) for existing turbojet engines; for fan-type jet engines this ratio may be as low as 35 lbf/lbm/sec (340 N/kg/sec), and for proposed lift-jet engines it may be as high as 90 lbf/lbm/sec (883 N/kg/sec). The data in figure 9 show that this factor can be simulated for values up to approximately 84 lbf/lbm/sec (824 N/kg/sec) by an ejector equipped with a 2-inch (5.08-cm) nozzle.

Effect of Variations of the Basic Ejector Configuration

The purpose of the second part of this investigation was to determine the effect of changes in the basic ejector configuration. The factors that were varied were nozzle exit area and shape, mixing-chamber length, deflection of both mixing chamber and nozzle exit, and inlet blockage.

Nozzle exit area.- The effect of varying the nozzle exit area is presented in figure 10. The exit area of the basic ejector configuration, 3.142 in^2 (20.272 cm^2), is used as the reference area. Three area ratios were tested: the reference area, 80 percent reference area, and 120 percent reference area. These data show that as the exit area increases, the total pressure in the entrance of the plenum chamber of the ejector and

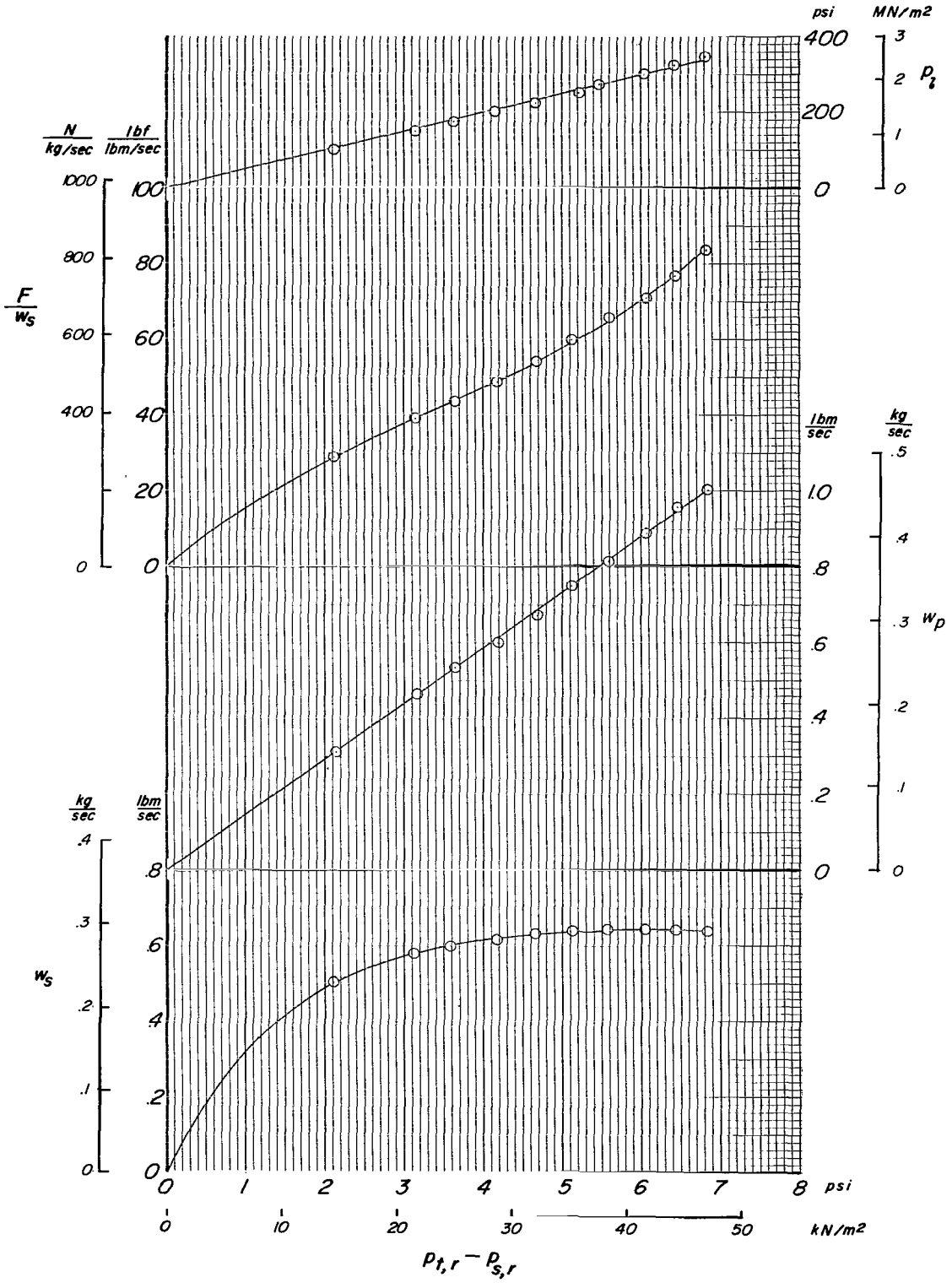

Figure 9.- Additional ejector performance characteristics.

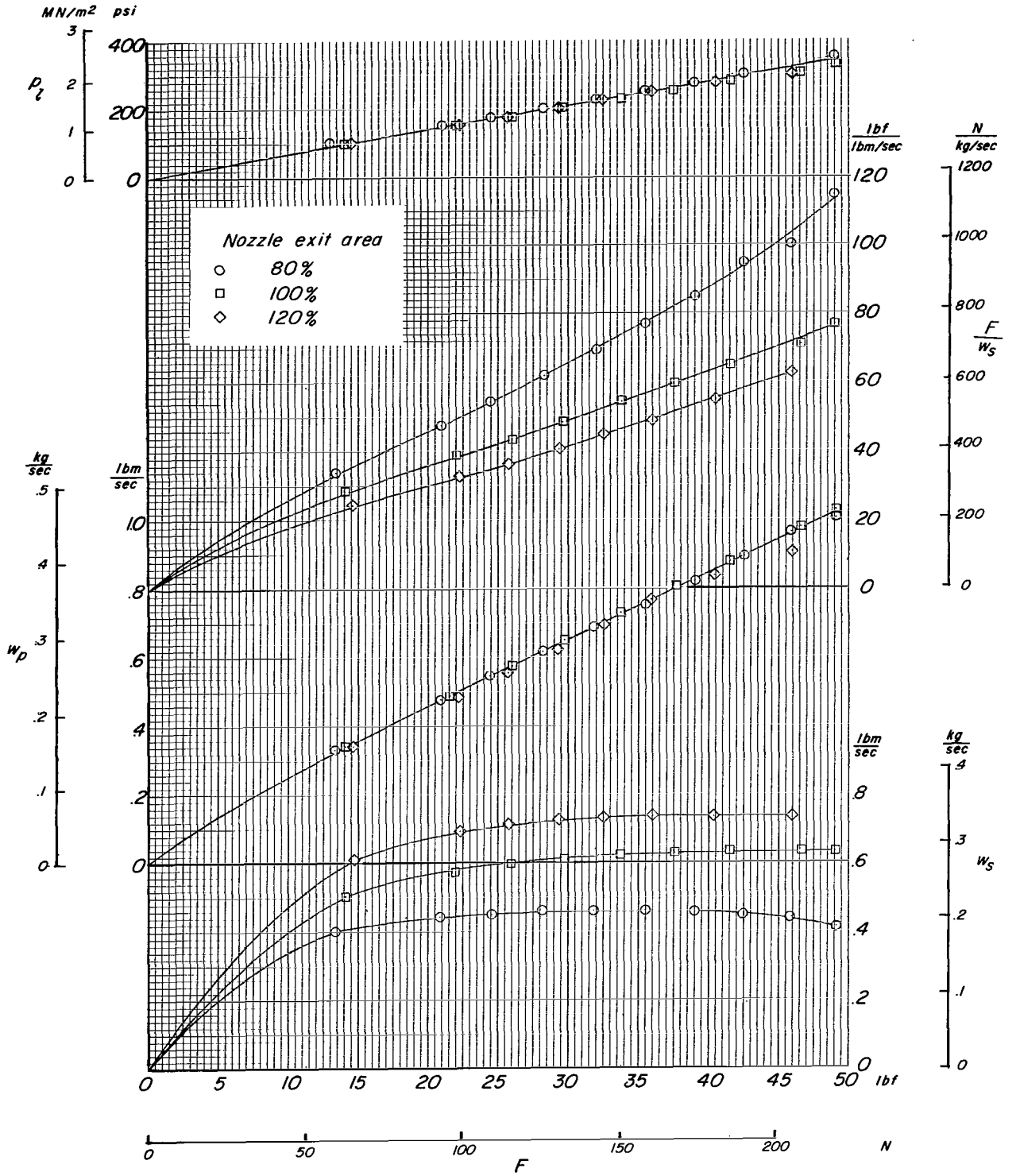

Figure 10.- Effect of exit area ratio on ejector performance.

the primary mass flow are unchanged for a given value of thrust, but the secondary mass flow increases. As a result, the scale factor (thrust divided by secondary mass flow) is reduced by an increase in exit area. Similarly, as the exit area decreases, the secondary mass flow decreases and the scale factor increases. Values as high as 115 lbf/lbm/sec (1128 N/kg/sec) can be obtained with the 80 percent exit area. Thus the scaling factor can be changed in two ways – by changing the value of thrust (varying the primary line pressure) or by changing the nozzle exit area.

Centerbody in the nozzle exit.- In most jet engines, there is a centerbody ahead of the nozzle exit, and consequently the exit is more annular than circular in cross section. The effect of the centerbody on the performance of the jet-engine simulator was investigated by testing the configuration sketched in figure 11. The results are compared with those for the basic ejector configuration in figure 12. Both nozzles have the same geometric exit area. It can be seen from these data that 15 percent additional primary-line total pressure and an additional increment of primary mass flow of about 0.14 lbm/sec (0.064 kg/sec) are required to achieve a particular value of thrust. The centerbody nozzle also has a reduced secondary mass flow. This increases the magnitude of the scale factor (thrust divided by secondary mass flow) by more than 40 percent, to values as high as 133 lbf/lbm/sec (1300 N/kg/sec).

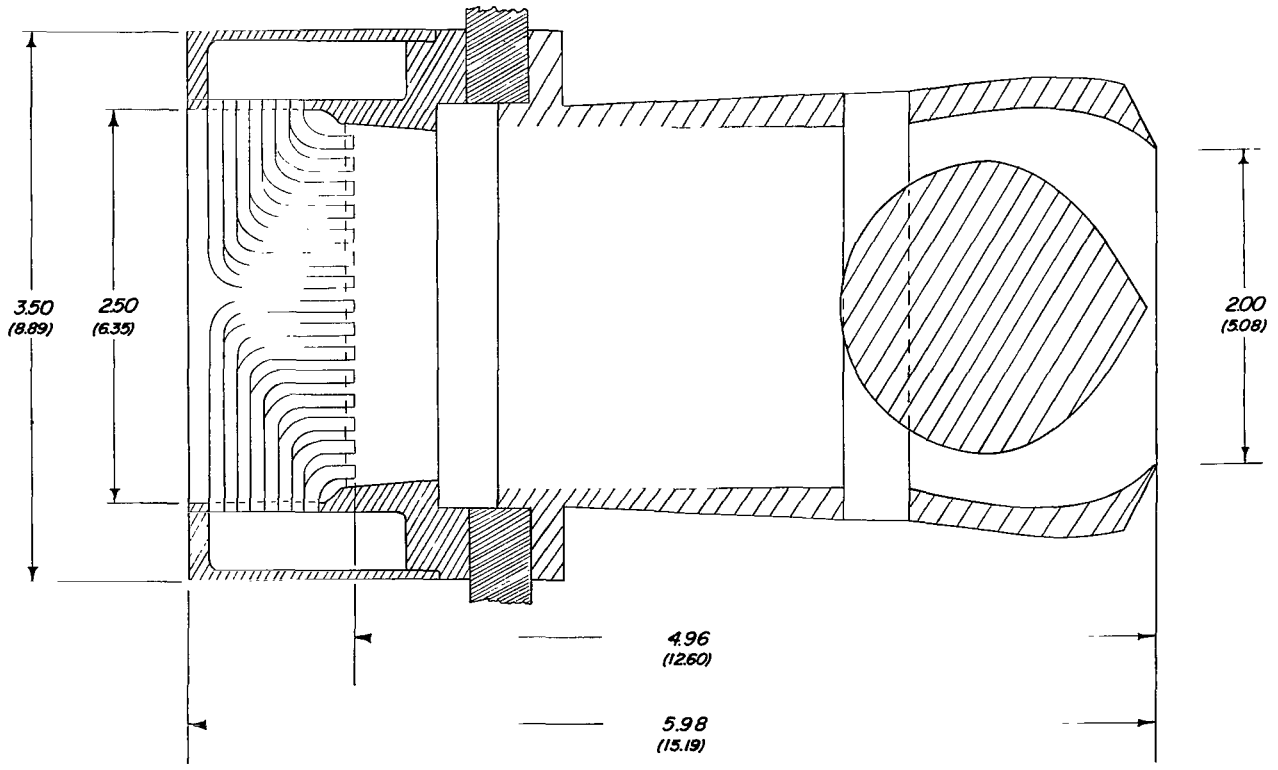

Figure 11.- Sketch of ejector with centerbody in the nozzle. Dimensions are in inches (centimeters).

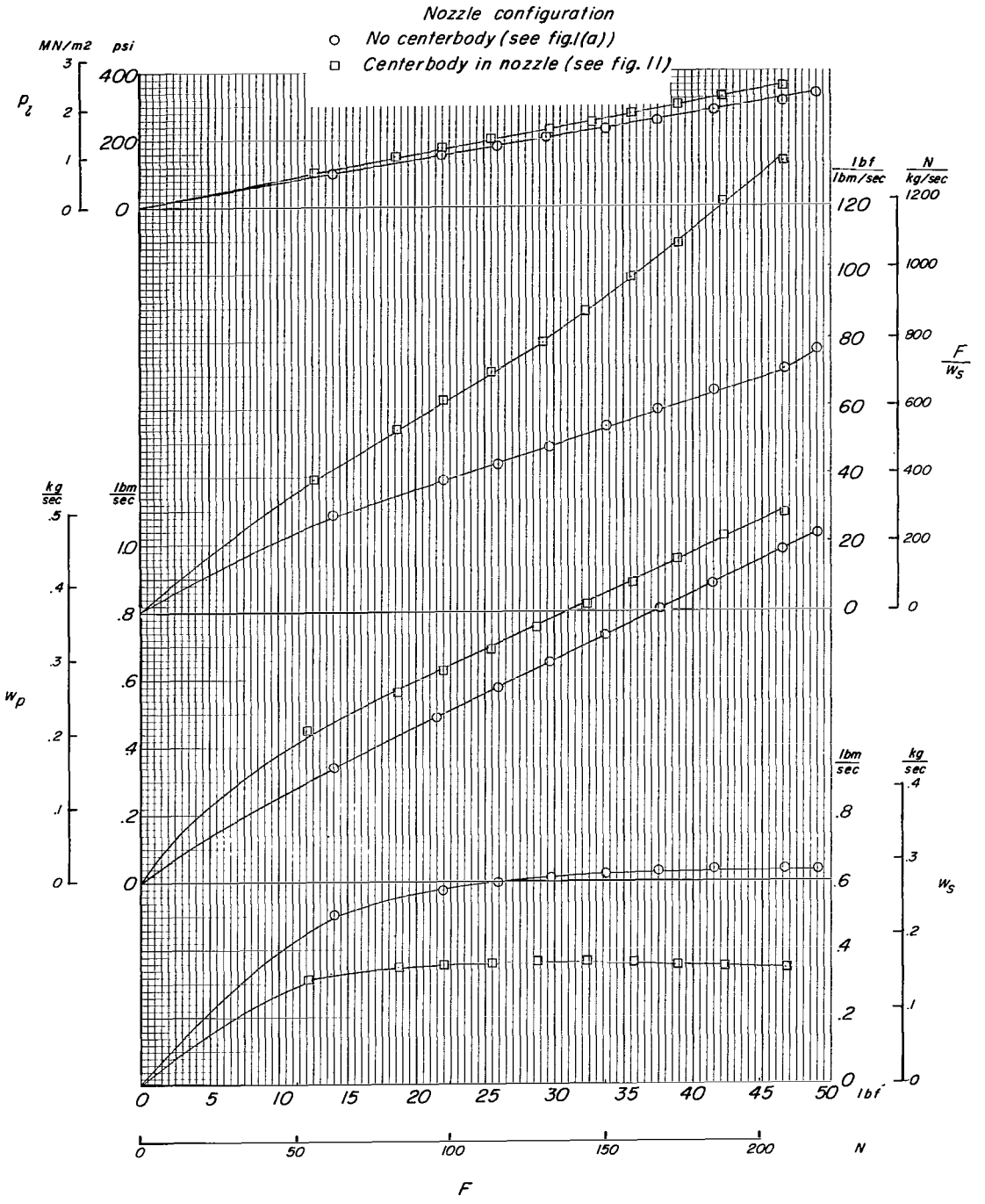

Figure 12.- Effect of centerbody in the nozzle on ejector performance.

Mixing-chamber length.- The effect of mixing-chamber length on the performance characteristics is presented in figure 13. No apparent change results when the nozzle length is increased from that of the basic ejector configuration, 1.45 exit-nozzle diameters, to 2.45 exit-nozzle diameters. The mixing-chamber length appears to be small when compared with the exit-nozzle diameter; however, when compared either with the throat diameter of one of the 177 primary nozzles or with the secondary area influenced by a single primary nozzle (1/177 of the area in the plane of the primary nozzle exits), the mixing length is quite large for both cases investigated. Once complete mixing is obtained, further increases in mixing length should have little effect on the measured thrust. The data in figure 13 indicate that the mixing is fairly complete in both these cases; therefore, even the shorter mixing chamber is adequate. An investigation (ref. 7) of a simple ejector with a single primary nozzle showed that when the area ratio A_p/A_j is low (below about 20), the length of the mixing chamber is not critical for good mixing of secondary and primary air. Since the ejector of the present investigation has an area ratio of 0.05, the results in figure 13 appear to be reasonable.

Deflection of the nozzle exit.- The effect of deflecting the nozzle exit is shown in figure 14 for the basic ejector configuration with deflections δ of 0^o, 15^o, and 30^o. These configurations represent simulated lift-jet engines. The resultant turning angles θ (fig. 14(a)) are very close to the nominal angles δ despite the fact that there are no turning vanes in the nozzles. The thrust presented is the value of the resultant thrust and is in the direction given by the turning angle. The thrust and the other data (fig. 14(b)) show that these nozzle deflections had little effect on the internal performance characteristics.

Deflection of both mixing chamber and nozzle exit.- The effect of deflecting the nozzle exit of an ejector configuration that simulates lift-cruise jet engines is presented in figure 15. For this configuration, the total mass flow is first turned by a 90^o elbow which contains a set of turning vanes, and then the air is turned by the exit nozzle to the desired deflection. As in the previous case, no turning vanes are used in the exit nozzle. The curves at the top of figure 15(a) show that the resultant deflection θ is lower than the intended angle δ of flow by up to 3^o. The resultant thrust and mass-flow data (fig. 15(b)) indicate that the nozzle deflection has little effect on the internal performance characteristics.

Blockage of the ejector inlet.- Tests were conducted with various amounts of solid blockage at the inlet to determine the effect of flow separation or distortion in the inlet of the jet-engine simulator on thrust and thrust calibration. The following five conditions were investigated: inlet open (100 percent of area open), inlet closed by a segment whose maximum perpendicular distance from the chord to the arc is D/4 (81.5 percent open), inlet half closed (50 percent open), inlet closed except for a segment whose maximum

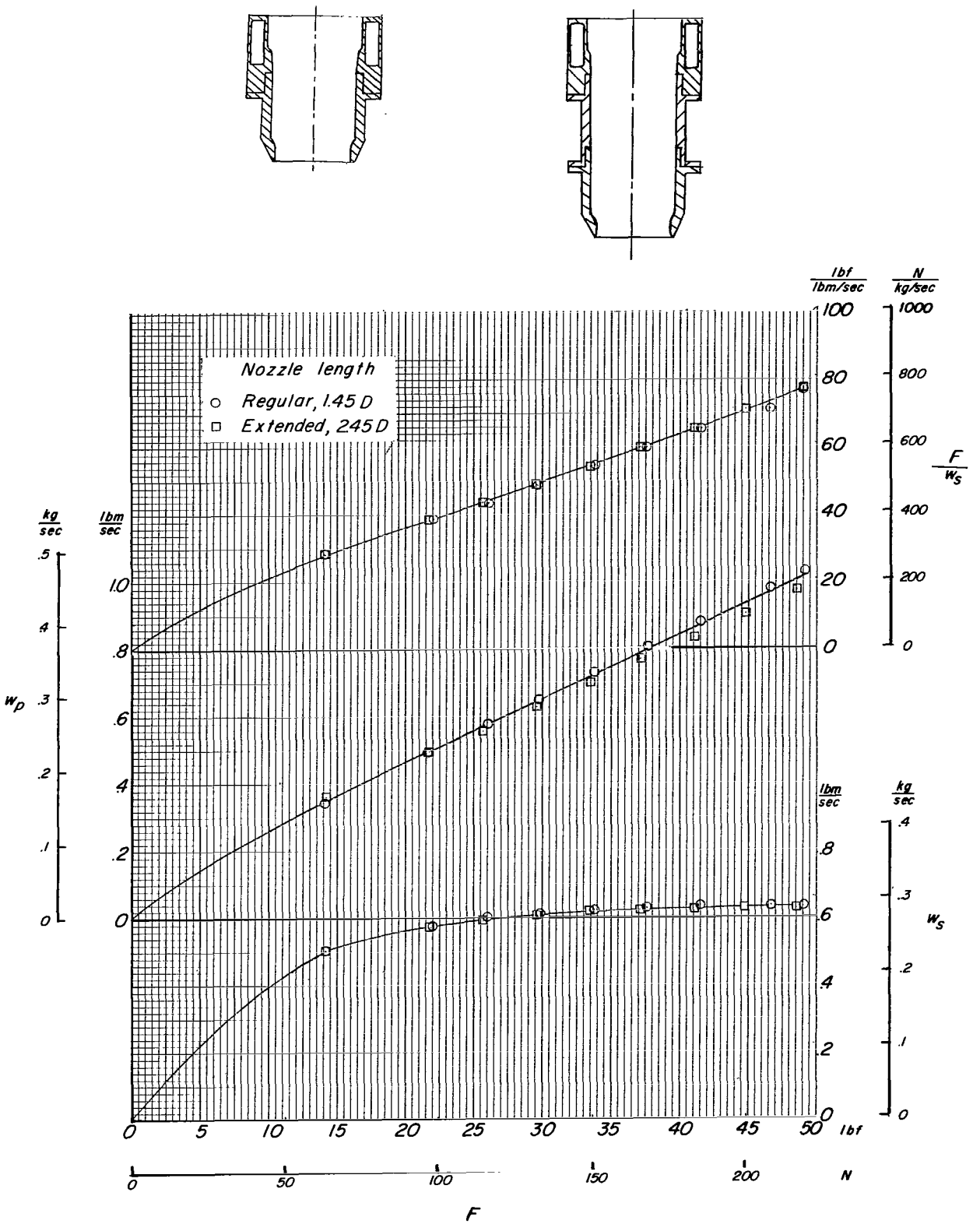

Figure 13.- Effect of mixing-chamber length on ejector performance.

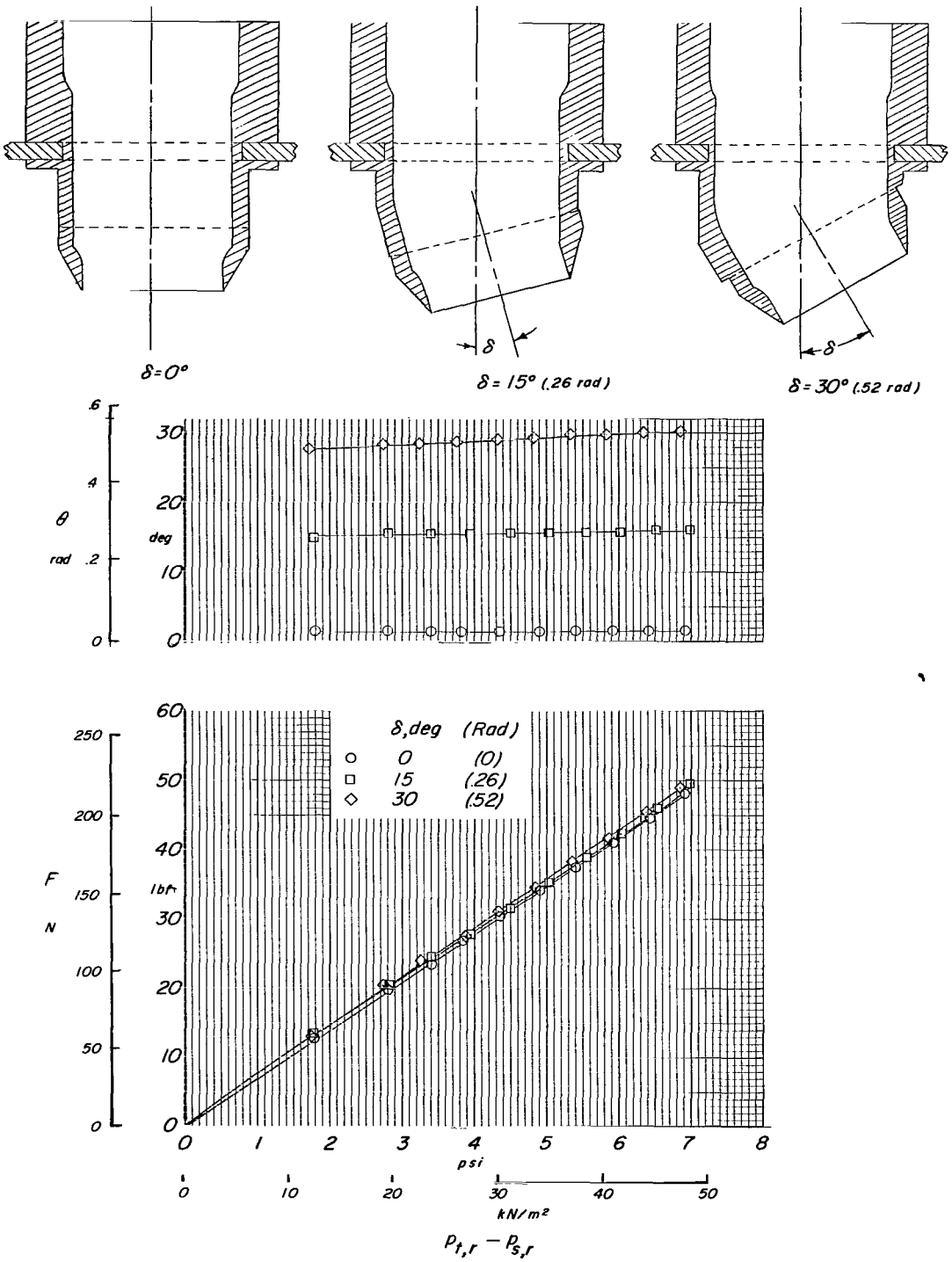

(a) Resultant thrust and deflection angles.

Figure 14.- Effect of nozzle deflection on lift engine simulator.

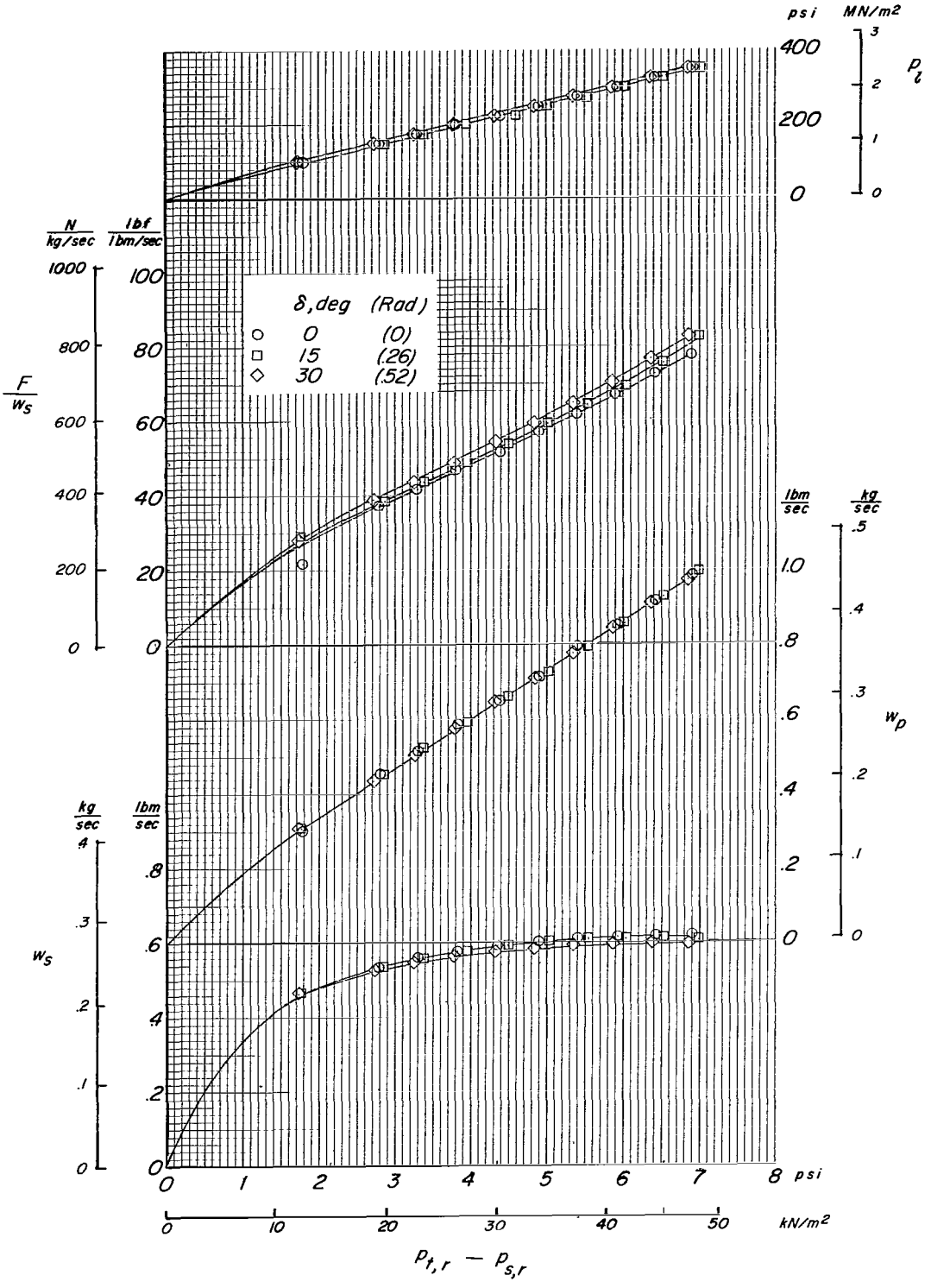

(b) Additional performance data.

Figure 14.- Concluded.

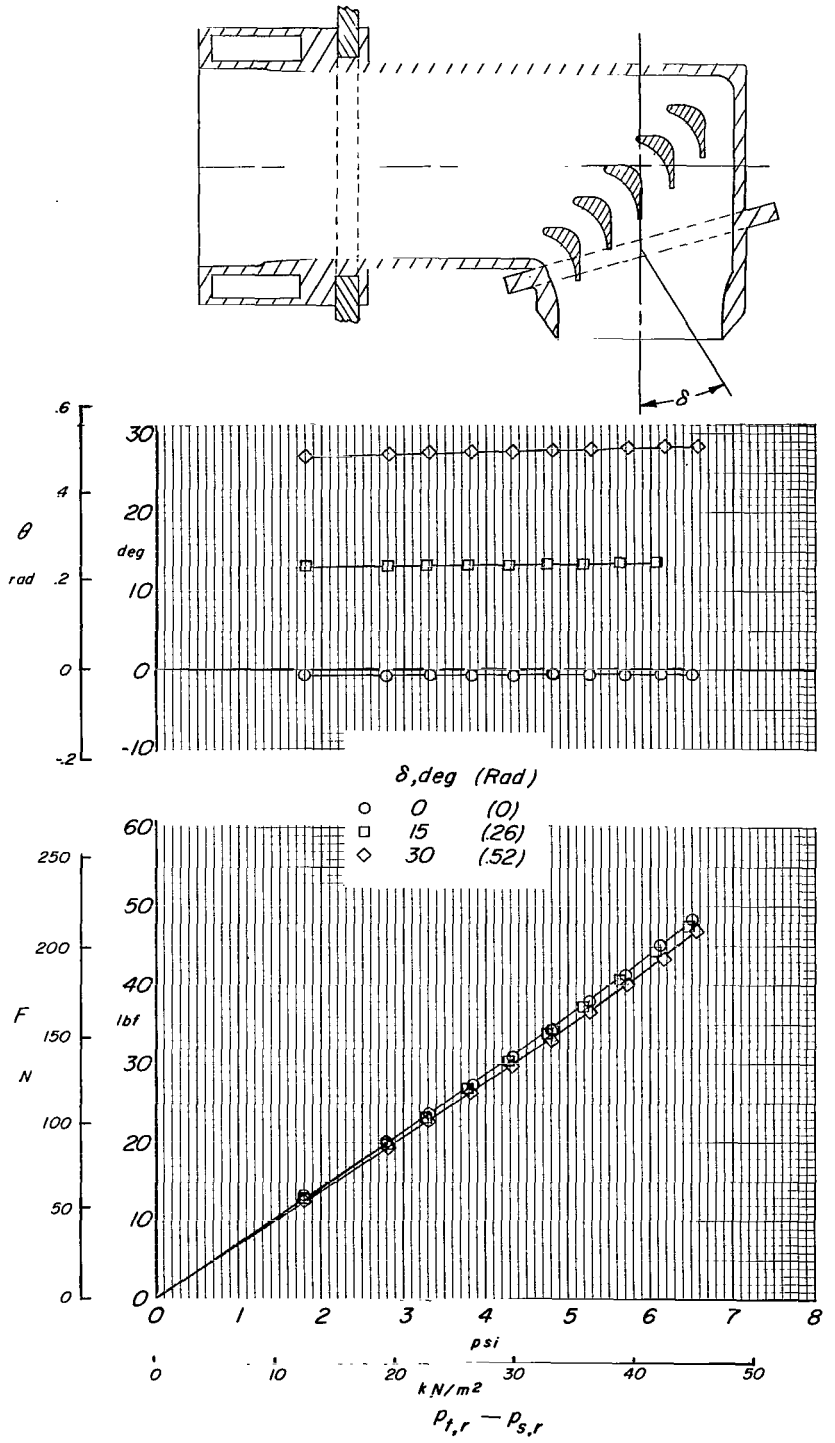

(a) Resultant thrust and deflection angles.

Figure 15.- Effect of nozzle deflection on lift-cruise engine simulator.

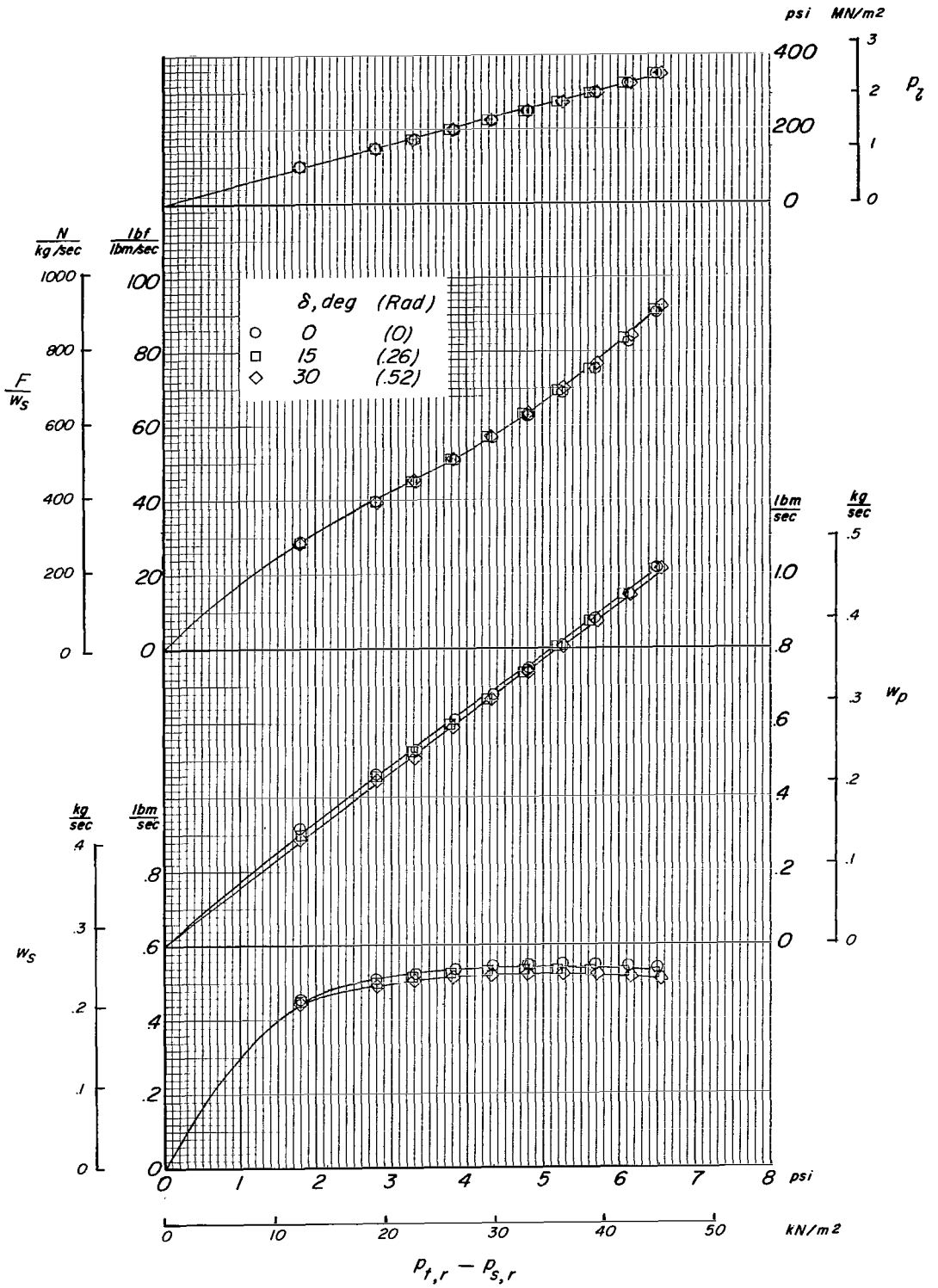

(b) Additional performance data.

Figure 15.- Concluded.

perpendicular distance from the chord to the arc is D/4 (18.4 percent open), inlet fully closed (0 percent open).

The thrust as a function of line pressure, presented in figure 16, shows a drastic reduction with increasing blockage. The difference between the curves for the fully open and closed inlets does not correspond to an augmentation of the thrust produced by the compressed air alone, because there are large suction pressures induced on the inside of the inlet blockage by the exit flow. These suction pressures impose a large download on the ejector and thus reduce the net thrust. Since the primary compressed-air nozzles cannot be operated without the annular plenum chamber around them, the augmentation cannot be determined experimentally. The information in reference 7 indicates that the augmentation ratio should be no higher than 1 for this ejector.

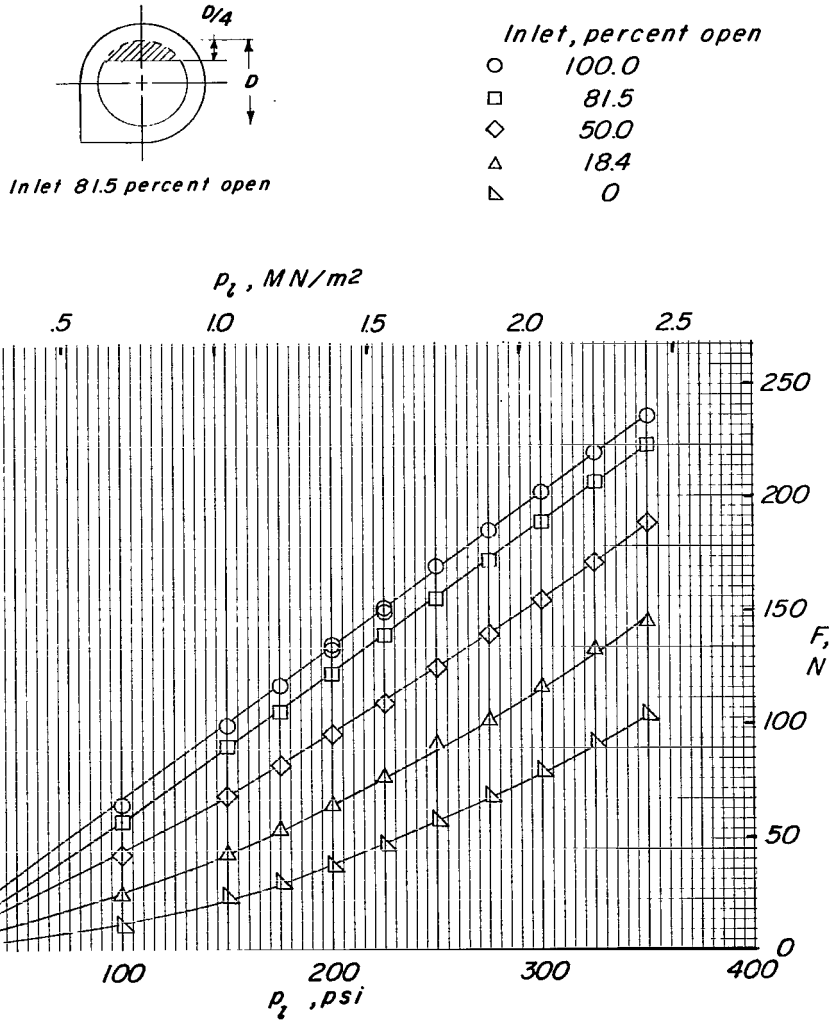

Figure 16.- Effect of inlet blockage on thrust as a function of line pressure.

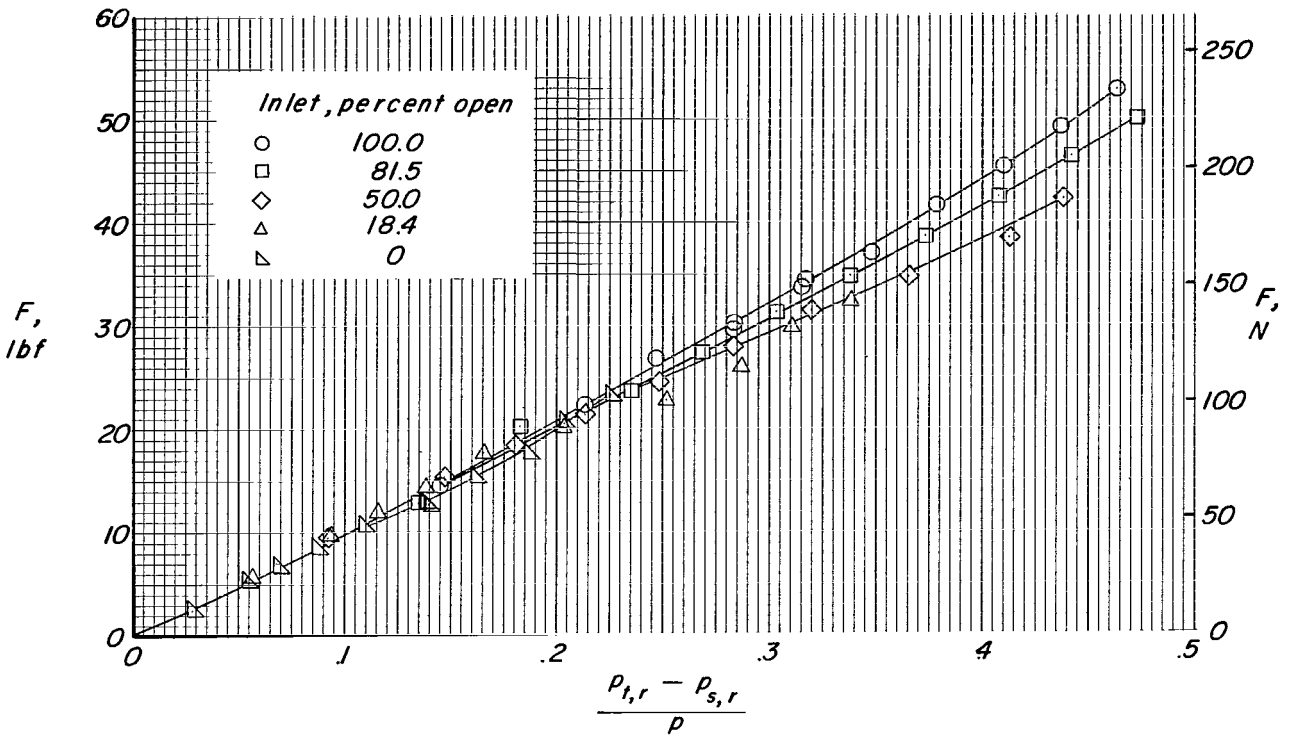

Figure 17.- Effect of inlet blockage on thrust as a function of pressure difference measured by the rake in the nozzle exit.

The effect of inlet blockage on the thrust calibration curve is presented in figure 17. The data do not give a single calibration curve. For the smallest blockage, there is as much as 6 percent reduction in thrust from that of the basic ejector configuration for a given pressure difference. The largest reduction in thrust is 15 percent and occurs with 50 percent blockage. Closing the inlet completely results in a reduction in thrust which ranges up to 8 percent. These data demonstrate the range of error in the thrust calibration when the jet-engine simulator is operated with the inlet blocked either partially or completely.

SUMMARY OF RESULTS

Static calibration of an ejector unit powered with compressed air has demonstrated the following performance characteristics:

1. Thrust can be determined from total-pressure and static-pressure measurements inside the ejector nozzle. Scatter of several calibrations for a single ejector and exit combination indicate that the thrust can be repeated within 1 percent for a given pressure difference in the exit.

2. Calibration of several ejectors and several nozzles indicates that each combination of ejector and nozzle exit has a different variation of thrust with exit pressure difference. Therefore, each combination used in a model must be calibrated separately.

3. Measurements of the induced lift loss of a single ejector are nearly the same as those given for the J-85 jet engines in NASA TN D-3435. Therefore, wind-tunnel models which use these ejectors should have levels of jet-induced lift loss that are comparable to those caused by a jet engine.

4. Data obtained by varying the nozzle exit area for a given ejector show that the secondary (inlet) mass flow is proportional to the exit area and that the thrust is relatively constant. As a result, values of the scale factor (ratio of jet thrust to secondary (inlet) mass flow) up to 84 lbf/lbm/sec (824 N/kg/sec) can be obtained with the 2.00-inch-diameter (5.08-cm) nozzle and values up to 115 lbf/lbm/sec (1128 N/kg/sec) can be obtained when the nozzle exit area is decreased to 80 percent of the basic area.

5. Deflection of the mixing chamber to provide nozzle angles up to 30^{o} affects only the wake angle of the jet. There is no significant effect on any of the other internal performance parameters.

6. Partial blockage of flow in the inlet to the ejector can change the ejector thrust calibration by as much as 15 percent. Complete blockage changed the ejector thrust calibration by as much as 8 percent.

Langley Research Center,
National Aeronautics and Space Administration,
Langley Station, Hampton, Va., October 19, 1966,
721-01-00-18-23.

REFERENCES

1. Williams, John; and Butler, Sidney F. J.: Further Developments in Low-Speed Wind-Tunnel Techniques for V/STOL and High-Lift Model Testing. Tech. Note No. Aero 2944, Brit. R.A.E., Jan. 1964.

2. Wood, M. N.; and Howard, J. B. W.: The Development of Injector Units for Jet-Lift Engine Simulation on Low-Speed-Tunnel Models. Tech. Rept. 65020, Brit. R.A.E., Feb. 1965.

3. Sacerdote, Ugo: Techniques for the Simulation of Jet-Lift Engines in Wind-Tunnel Models of V/STOL Aircraft. Aerodynamics of Power Plant Installation, Part II, AGARDograph 103, Oct. 1965, pp. 587-617.

4. Mechtly, E. A.: The International System of Units – Physical Constants and Conversion Factors. NASA SP-7012, 1964.

5. Gentry, Garl L.; and Margason, Richard J.: Jet-Induced Lift Losses on VTOL Configurations Hovering In and Out of Ground Effect. NASA TN D-3166, 1966.

6. McLemore, H. Clyde: Jet-Induced Lift Loss of Jet VTOL Configurations in Hovering Condition. NASA TN D-3435, 1966.

7. Wan, Chia-An: A Study of Jet Ejector Phenomena. AIAA Student J., vol. 3, no. 3, Oct. 1965, pp. 77-86.

"The aeronautical and space activities of the United States shall be conducted so as to contribute . . . to the expansion of human knowledge of phenomena in the atmosphere and space. The Administration shall provide for the widest practicable and appropriate dissemination of information concerning its activities and the results thereof."

—NATIONAL AERONAUTICS AND SPACE ACT OF 1958

NASA SCIENTIFIC AND TECHNICAL PUBLICATIONS

TECHNICAL REPORTS: Scientific and technical information considered important, complete, and a lasting contribution to existing knowledge.

TECHNICAL NOTES: Information less broad in scope but nevertheless of importance as a contribution to existing knowledge.

TECHNICAL MEMORANDUMS: Information receiving limited distribution because of preliminary data, security classification, or other reasons.

CONTRACTOR REPORTS: Technical information generated in connection with a NASA contract or grant and released under NASA auspices.

TECHNICAL TRANSLATIONS: Information published in a foreign language considered to merit NASA distribution in English.

TECHNICAL REPRINTS: Information derived from NASA activities and initially published in the form of journal articles.

SPECIAL PUBLICATIONS: Information derived from or of value to NASA activities but not necessarily reporting the results of individual NASA-programmed scientific efforts. Publications include conference proceedings, monographs, data compilations, handbooks, sourcebooks, and special bibliographies.

Details on the availability of these publications may be obtained from:

SCIENTIFIC AND TECHNICAL INFORMATION DIVISION

NATIONAL AERONAUTICS AND SPACE ADMINISTRATION

Washington, D.C. 20546